Physical and genetic map of the *Spiroplasma kunkelii* CR2-3x chromosome

Ellen L. Dally, Thereza S.L. Barros, Yan Zhao, ShaoPing Lin, Bruce A. Roe, and Robert E. Davis

Abstract: *Spiroplasma kunkelii* (class *Mollicutes*) is the characteristically helical, wall-less bacterium that causes corn stunt disease. A combination of restriction enzyme analysis, pulsed-field gel electrophoresis (PFGE), and Southern hybridization analysis was used to construct a physical and genetic map of the *S. kunkelii* CR2-3x chromosome. The order of restriction fragments on the map was determined by analyses of reciprocal endonuclease double digests employing I-*Ceu*I, *Asc*I, *Apa*I, *Eag*I, *Sma*I, *Bss*HII, *Bgl*I, and *Sal*I; adjacent fragments were identified on two-dimensional pulsed-field electrophoresis gels. The size of the chromosome was estimated at 1550 kb. Oligonucleotide pairs were designed to prime the amplification of 26 *S. kunkelii* gene sequences in the polymerase chain reaction (PCR). Using PCR amplicons as probes, the locations of 27 *S. kunkelii* putative single-copy genes were positioned on the map by Southern hybridization analyses of chromosomal fragments separated in PFGE. The nucleotide sequence of the single ribosomal RNA operon was determined and its location mapped to a chromosomal segment bearing recognition sites for *Sal*I, *Sma*I, *Eag*I, and I-*Ceu*I.

Key words: Spiroplasma kunkelii CR2-3x, corn stunt spiroplasma, mollicutes, genome mapping, two-dimensional pulsed-field gel electrophoresis.

Résumé : *Spiroplasma kunkelii* (classe *Mollicutes*) est une bactérie sans parois d'aspect hélicoïdal qui cause la maladie du rabougrissement du maïs. Une combinaison d'analyses par enzymes de restriction, d'électrophorèse sur gel en champs pulsé (PFGE) et d'analyses par hybridation de type Southern fut employée afin de construire une carte physique et génétique du chromosome de la souche CR2-3x de *S. kunkelii*. L'ordre des fragments de restriction dans la carte fut déterminé en analysant la double digestion d'endonucléases réciproques, utilisant pour ce faire I-*Ceu*I, *Asc*I, *Apa*I, *Eag*I, *Sma*I, *Bss*HII, *Bgl*I et *Sal*I; les fragments adjacents furent identifiés sur des gels d'électrophorèse en champs pulsé bidimensionnel. La taille du chromosome fut estimée à 1550 kb. Des paires d'oligonucléotides furent conçues afin d'amorcer l'amplification de la séquence de 26 gènes de *S. kunkelii* par réaction de la polymérase en chaîne (PCR). En employant les amplicons de PCR en tant que sondes, les localisations de 27 gènes putatifs à copie unique de *S. kunkelii* furent positionnées dans la carte par analyses d'hybridation de type Southern de fragments chromosomiques séparés par PFGE. La séquence nucléotidique de l'opéron d'ARN ribosomal unique fut déterminée et sa localisation chromosomique fut cartographiée à un segment chromosomique renfermant les sites de reconnaissance de *Sal*I, *Sma*I, *Eag*I et I-*Ceu*I.

Mots clés : Spiroplasma kunkelii CR2-3x, spiroplasmes du rabougrissement du maïs, mollicutes, électrophorèse sur gel en champ pulsé bidimensionnel.

[Traduit par la Rédaction]

Received 7 February 2006. Revision received 13 April 2006. Accepted 19 April 2006. Published on the NRC Research Press Web site at http://cjm.nrc.ca on 27 September 2006.

E.L. Dally, Y. Zhao, and R.E. Davis.[1] USDA, Agricultural Research Service, Molecular Plant Pathology Laboratory, Beltsville, MD 20705, USA.
T.S.L. Barros.[2] USDA, Agricultural Research Service, Molecular Plant Pathology Laboratory, Beltsville, MD 20705, USA; Laboratório de Virologia e Microscopia Eletrônica, Departamento de Biologia Celular, Universidade de Brasília, Brasília, DF 70919-970, Brazil.
S.P. Lin and B.A. Roe. Advanced Center for Genome Technology, Department of Chemistry and Biochemistry, University of Oklahoma, Norman, OK 73019, USA.

[1]Corresponding author (e-mail: davisr@ba.ars.usda.gov).
[2]USDA, Animal Plant Health Inspection Service, US Embassy, Av. Das Nacoes Sul, Quadra 801, lote 03, CEP 70403-900, Brasília-DF, Brazil.

 doi:10.1139/W06-044

Introduction

Members of the genus *Spiroplasma* (class *Mollicutes*) are characteristically helical, wall-less bacteria. First discovered in diseased plants (Davis and Worley 1973; Davis et al. 1972), currently known spiroplasmas comprise broadly diverse species infecting plants, insects, ticks, freshwater crustaceans, and a marine shrimp (Hackett and Clark 1989; Nunan et al. 2005; Wang et al. 2004, 2005). Like other mollicutes, spiroplasmas are thought to have descended from low G+C Gram-positive clostridium-like eubacterial ancestors by degenerative or reductive evolution that resulted in significant losses of genomic sequences and biochemical capabilities (Woese et al. 1980) and in small genome size (940–2200 kb) (Carle et al. 1995).

Corn stunt disease caused by *Spiroplasma kunkelii* is a major limiting factor in the production of corn (maize, *Zea mays* L.) in the Americas (Davis et al. 1981; Giménez Pecci et al. 2002; Hruska and Gomez Peralta 1997; Nault 1990; Oliveira et al. 2003; Whitcomb et al. 1986). *Spiroplasma kunkelii* is transmitted in a persistent, propagative manner from diseased to healthy corn plants by phloem-feeding leafhoppers. In nature, the major insect vectors of *S. kunkelii* are *Dalbulus maidis* (DeLong and Wolcott) and *Dalbulus elimatus* (Ball) (Davis et al. 1981; Nault 1990). In diseased corn, the spiroplasma resides in phloem sieve cells and induces symptoms of severe stunting, tillering, broad chlorotic striping of leaves, sterility in tassels, poorly filled ears, and sometimes, reddening of leaves. Control measures for corn stunt disease currently include planting of resistant corn hybrids, controlling insect vector populations by use of insecticides or by other measures, and adjusting planting dates (Hruska and Gomez Peralta 1997; Summers and Stapleton 2002).

Although *S. kunkelii* is an agriculturally important pathogen exhibiting trans-kingdom parasitism, parasitizing both plant and insect hosts, relatively little is known about its biochemistry, genetics, and physiology. To gain new insights into the basic biological processes and mechanisms of survival, host adaptation, and pathogenicity of this prokaryote, a collaborative project was initiated to sequence, assemble, and annotate the entire genome of *S. kunkelii* CR2-3x (http://www.genome.ou.edu/spiro.html and http://www.barc.usda.gov/psi/mppl/spiroplasma/index.html). Several reports using the publicly available sequence data generated in the project have recently been published (Bai et al. 2004*a*, 2004*b*; Davis et al. 2005; Zhao et al. 2003, 2004*a*, 2004*b*, 2005), providing new knowledge of cellular processes, metabolism, gene organization, and pathogenicity of *S. kunkelii*.

Here, we describe the construction of a physical and genetic map of *S. kunkelii* CR2-3x chromosome by using restriction enzyme analyses, one- and two-dimensional (2-D) pulsed-field gel electrophoresis (PFGE), and Southern hybridization analyses. The map will contribute to a general understanding of the organization of the *S. kunkelii* genome, provide a basis for comparative genome analysis with other spiroplasma chromosomes, and contribute to an understanding of spiroplasma evolution.

Materials and methods

Spiroplasma culture and DNA extraction

Spiroplasma kunkelii CR2-3x, originally isolated from naturally infected corn plants in Costa Rica, was triply cloned and verified for insect transmission and was kindly supplied by Dr. Jacqueline Fletcher at Oklahoma State University, Stillwater. The strain was grown in serum-containing medium LD8A3 (Lee and Davis 1989) at 30 °C to a concentration of ~5 × 10^8 cells/mL. Total genomic DNA for use in conventional agarose gel electrophoresis and in polymerase chain reactions (PCR) was isolated from cells according to the previously published procedure of Lee and Davis (1980).

Preparation of genomic DNA for PFGE

Spiroplasma kunkelii cells were embedded in agarose, lysed, and deproteinized as described by Neimark and Kirkpatrick (1993) with some modifications. The cell culture (~5 × 10^8 cells/mL) was pelleted by centrifugation (12 000*g*, 35 min), washed once in sterile TS buffer (20 mmol/L Tris–HCl, pH 8.0, 10% sucrose), and resuspended in TS at a 10-fold concentration relative to the original culture. Cell suspensions were warmed briefly at 37 °C and quickly mixed with an equal volume of 2% agarose (Low Melt Preparative Grade Agarose, Bio-Rad Laboratories, Hercules, Calif.) in 2× TES buffer (0.2 mol/L Tris–HCl, 0.2 mol/L NaCl, 20 mmol/L EDTA, pH 8.0), which had been previously melted and maintained at 45 °C. The mixture was rapidly dispensed into ice-cold disposable plastic molds (Bio-Rad Laboratories) and allowed to solidify for 30 min. Each agarose block contained 75 µL of the cell–agarose mixture. The solidified agarose blocks were removed from the molds and incubated in prewarmed lysis buffer (0.5 mol/L EDTA, pH 8.0, 1% SDS; 100 blocks in 30 mL), supplemented with 1 mg/mL proteinase K (Invitrogen, Carlsbad, Calif.), at 52 °C for 72 h, with a change of lysis buffer every 24 h. The SDS–lysis solution was then replaced with prewarmed sarkosyl–EDTA solution (1% *N*-laurylsarcosine, 0.5 mol/L EDTA, pH 8.0), and the blocks were incubated for 1 h at 52 °C before long-term storage at 4 °C. Before restriction endonuclease digestion, blocks were washed four times with 1× TE buffer (10 mmol/L Tris–HCl, pH 8.0, 1 mmol/L EDTA) at room temperature for 1 h each time.

Restriction endonuclease digestion of genomic DNA

Agarose blocks containing *S. kunkelii* genomic DNA were digested with restriction endonucleases, including *Apa*I, *Asc*I, *Bgl*I, *Bss*HII, *Eag*I, *Sma*I, and *Sal*I (New England BioLabs, Beverly, Mass.), and with I-*Ceu*I, according to the manufacturer's guidelines. Three to five blocks were placed in a sterile 2 mL microcentrifuge tube and equilibrated with 1 mL of the appropriate restriction enzyme buffer supplemented with 100 µg/mL of bovine serum albumin for 2 h on ice. Then 40–60 U of restriction enzyme was added to each tube, and the blocks were allowed to equilibrate on ice for another 2 h before incubating at the appropriate reaction temperature overnight (16–18 h). Additional restriction enzyme was added to each tube (half the initial amount), and the blocks were incubated for five more hours. The digestions were stopped by rinsing the blocks in 1× TE buffer. Double digestions were performed sequentially. For double digestions analyzed by 2-D PFGE, agarose strips containing the DNA fragments after digestions with one enzyme and electrophoresis in one dimension were excised from the gel, washed with 1× TE, placed in sterile tubes, and equilibrated with the appropriate buffer for 16 h. After equilibration with 150–200 U of

enzyme for 2 h on ice, the DNA fragments were digested for 16–18 h, and then additional enzyme (half the initial amount) was added and incubation continued for five more hours. After enzyme digestions, agarose blocks and strips were stored at 4 °C in 1× TE prior to PFGE. Predictions of the numbers of recognition sites were calculated as described (Ye et al. 1992).

PFGE

PFGE was performed in a contour-clamped homogeneous electric field apparatus (CHEF-DR III, Bio-Rad Laboratories) following the manufacturer's guidelines. Agarose gels (1% Pulsed-Field Certified Agarose, Bio-Rad) were run in 0.5× TBE (44.5 mmol/L Tris–HCl, 44.5 mmol/L boric acid, 1 mmol/L EDTA, pH 8.0) at 14 °C, constant voltage (6 V/cm), and 120° reorientation angle, with switch times and run times varying according to the size range of fragments being separated. The sizes of separated fragments were estimated by comparing mobilities of the bands with those of DNA molecular size standards for PFGE (Low Range PFG Marker, MidRange I PFG Marker, MidRange II PFG Marker, Lambda Ladder PFG Marker, and Yeast Chromosome PFG Marker; New England BioLabs). Gels were stained in ethidium bromide (0.5 μg/mL) for 30 min, destained in water for 30 min, and photographed under ultraviolet (UV) light.

Two-dimensional PFGE was carried out as described by Bautsch (1988) and Birren and Lai (1993). The double digestions with different enzymes for the 2-D PFGE were performed sequentially, as described above. The DNA fragments cut from the first pulsed-field (PF) gel were digested by the second restriction enzyme, cast in a second gel, and run under conditions compatible with separating the smaller restriction fragments expected from the second digestion. Fragments resulting from the single and double enzyme digestions of DNA in blocks were also included for analysis by 2-D PFGE. Linking fragments on the map were identified as described by Bautsch (1988). The order of the restriction fragments on the chromosome was determined by analyses of sequential, reciprocal double digests analyzed in the 2-D PF gels.

Spiroplasma kunkelii genomic DNA probes

Spiroplasma kunkelii genes of interest for use as hybridization probes were identified from the publicly available nucleotide sequence data of the *Spiroplasma kunkelii* Strain CR2-3x Genome Sequencing Project at http://www.genome.ou.edu/spiro.html. A primer pair for use in PCR was designed to amplify a portion of each gene; PCR was carried out as previously described (Barros et al. 2001), except that the annealing temperature used was 55 °C. Genes and PCR primers are listed in Table 1. Probes were prepared by random-primed labeling of PCR products with digoxigenin (DIG), using the DIG-High Prime Labeling Kit (Roche Applied Science, Indianapolis, Ind.), according to the manufacturer's directions.

Southern blot hybridization analysis

DNA fragments in PF gels were transferred onto positively charged nylon membranes (Roche), hybridized with DNA probes, and hybridizations were detected by standard procedures (Maniatis et al. 1982) with some modifications. After electrophoresis and staining in ethidium bromide, DNA fragments in PF gels were exposed to a total of 60 mJ of UV energy in a Stratalinker UV Crosslinker (Stratagene, La Jolla, Calif.) to facilitate the transfer of high molecular weight DNA during blotting. Following denaturation and neutralization, the DNA fragments were transferred to nylon membranes in 20× SSC (3 mol/L NaCl, 0.3 mol/L sodium citrate, pH 7.0) for 48 h and were bound to the membrane by UV cross-linking. Membranes were incubated with DIG-labeled DNA probes. Prehybridization and hybridization with the probe were performed at 42 °C in the presence of 50% formamide, 5× SSC, 5% SDS, 5% sarkosyl, and 5% blocking reagent (Roche). After a 16 h hybridization period, the membranes were washed two times in 2× SSC with 0.1% SDS at room temperature for 15 min each time, followed by two high stringency washes in 0.5× SSC with 0.1% SDS at 50 °C for 25 min each. Filter blocking was performed at room temperature for 4 h in blocking solution (2% blocking reagent, 0.1 mol/L maleic acid, 0.15 mol/L NaCl, pH 7.5). The hybridization signal was detected by a colorimetric assay with anti-DIG alkaline phosphatase-conjugated Fab fragment (Roche) with nitroblue tetrazolium (Roche) and 5-bromo-4-chloro-3-indolyl phosphate (Roche) as substrates, according to the manufacturer's guidelines. Each gene was located on the physical map by identifying the overlapping restriction fragments detected in the hybridization.

Results

Undigested high molecular weight genomic DNA did not migrate in PFGE, indicating that *S. kunkelii* CR2-3x possessed a circular chromosome, as suggested for that of *Mycoplasma pneumoniae* by Krause and Mawn (1990). A low-intensity single band was occasionally observed in addition to unmigrated DNA; results from hybridization experiments, using total *S. kunkelii* DNA as a probe, indicated that the band was spiroplasma chromosomal DNA probably linearized by random breakage. The size of the spiroplasma chromosome was estimated at 1600 kb.

Restriction analysis of chromosomal DNA and size of the chromosome

High molecular weight spiroplasma DNA was digested with 25 restriction endonucleases to determine which enzymes produced a small number of fragments well-separated by PFGE and, therefore, were useful for mapping the chromosome. Since *S. kunkelii* DNA has a low G+C content (~26 mol%), restriction enzymes that have recognition sites high in G+C were chosen for this screening. Compared with undigested DNA, digestions with *Asc*I (recognition site, GGCGCGCC) and I-*Ceu*I (recognition site, TAACTATAACGGTCCTAAGGTAGCGA) resulted in a significant increase in the intensity of the band that migrated at 1600 kb on PF gels. This result indicated that the spiroplasma chromosome was circular and contained a single site for each of these two enzymes. *Not*I (recognition site, GCGGCCGC) and *Fse*I (recognition site, GGCCGGCC) did not cut the *S. kunkelii* CR2-3x chromosome.

Restriction enzymes chosen for constructing the map included *Apa*I (recognition site, GGGCCC), *Eag*I (CGGCCG),

Table 1. *Spiroplasma kunkelii* genes and polymerase chain reaction (PCR) primers used in generating probes for constructing the genetic map.

Gene designation	Gene product and (or) predicted function	PCR primer 1	PCR primer 2
argS	Arginyl-tRNA synthetase	5′-TTGCTGCTCCTTCAATGCAACG-3′	5′-GGTCATGCTCGGAATGGTGCCATTGC-3′
amyA	α-Amylase	5′-CGCTAAAGCTGTAGCTGATTC-3′	5′-CAAGAAGCGATTGTGTATGAAA-3′
parC	DNA topoisomerase IV subunit A	5′-GCAGAGTTTCCACTGTTGTTAC-3′	5′-GCACGTGCACAAAAACGCTCAG-3′
rrn	16S–23S ribosomal RNA operon (partial)	5′-GAGAGTTTGATCCTGGCTCAGGAT-3′	5′-ATTCCCAAGGCATTCACCATACG-3′
SKnhm	Hypothetical protein	5′-CAGGCAATCTTGATAGGAGCAC-3′	5′-TAAAACCTAAGACCCTATTC-3′
gapN	NADP-dependent glyceraldehyde-3-phosphate dehydrogenase	5′-GGTCCTCGTTGAGTACGACCATTA-3′	5′-GTCATAAGACAGAGATTGCGAAAA-3′
SK98-36	Hypothetical protein	5′-CTACCAGTATAGTATTCTGAT-3′	5′-TTGCCAGTTGAAGTAGCTGG-3′
secY	Preprotein translocation channel	5′-GACTCGCCATAATCGCGAGGTTG-3′	5′-GGTAAGAAGGGACGGGTTTC-3′
gpm	Phosphoglycerate mutase	5′-GGTGATGGACGTGATACGAAACC-3′	5′-CAGCATTTCCGTGGTCAGCAGTA-3′
SK99-22	Hypothetical protein	5′-GTAAGCATAGTAGCCAACTGCGCC-3′	5′-AGGACTTAGCATCAGTGGCTTAA-3′
SKvmp	Hypothetical protein	5′-CGCGACTATCGCAGGGATCGG-3′	5′-CATCTAATCCGGCTAGTTCGGC-3′
eno	Enolase	5′-CACCTTCTTTGCCTGGTTTAT-3′	5′-TTGAACAGAATTTGGCGG-3′
leuS	Leucyl-tRNA synthetase	5′-CATCGTATTAGTTTCTCGGCGTCC-3′	5′-GGATTAGCTGAGATGCGTGATG-3′
fruK	1-Phosphofructokinase	5′-ATGATGTCGCTGATCCAGCAC-3′	5′-GCATTAGGCTTTTTGGGGCGTG-3′
smc	Chromosome segregation ATPase	5′-GAGCAAGCAATTGTGACTGCTT-3′	5′-TGTCTTAGCATGGTCATATGTC-3′
lemA	Cytoplasmic membrane protein	5′-ATGAGATATAATCCAACAGT-3′	5′-CATCTTGACGATCAGCAGCA-3′
ffh	Signal recognition particle M54 protein	5′-TTTGGCATACGCCCTGATTT-3′	5′-CAACCTTAACGACTGATGCTA-3′
thrS	Threonyl-tRNA synthetase	5′-AGAAACAGGGGCAGAACAAGCCGG-3′	5′-GCTTCCCGATGTCTCATAACGATG-3′
pnp	Polynucleotide phosphorylase	5′-TGTTGAGCATGGCCAATTAGC-3′	5′-GCACTCCAGCCGCCATTAGAG-3′
secA	Preprotein translocation motor	5′-GATCACGTCGTGCATACATTGC-3′	5′-CTGGCCGTTTAATGCCGGGGCGTG-3′
rpoB	DNA-directed RNA polymerase, subunit B	5′-TCGTGATGGTACCCCTAATGGA-3′	5′-CAGGGATTAGCGAAGTGTTCGG-3′
folD	5,10-Methylenetetrahydrofolate dehydrogenase	5′-GCAACGTCTACCTGCCTTAAC-3′	5′-TTAGCTTTCCCCAAGGCAGAA-3′
fhs	Formate-tetrahydrofolate ligase	5′-TTAGCCATACAAACTGGTC-3′	5′-TCCAACCAAACCAGGAGAGGG-3′
thyA	Thymidylate synthase	5′-GGTAATTTTCGCGGAGAACGTG-3′	5′-GATGATCGAACAAATACGGG-3′
Spiralin*	Spiralin	5′-CTGTAGCGGCAAAAGATGTA-3′	5′-AGTAGTTGCGGCTGAATAGTT-3′
dnaA	Chromosomal replication initiation protein	5′-TGCTAATTGTCGTGCTTGCA-3′	5′-ATGAATCAGTTTCCCAGAA-3′
gyrA	DNA-gyrase, subunit A	5′-CTTCATCACCATTTACAGCTTGAAC-3′	5′-AGTAGTTGAACAAGCATGAGC-3′

*Spiralin gene primer sequences were from Barros et al. (2001).

Fig. 1. Pulsed-field gel electrophoresis of high molecular weight genomic DNA from *Spiroplasma kunkelii* CR2-3x digested with restriction endonucleases *Eag*I (Ea), *Bss*HII (Bs), *Sal*I (Sl), *Sma*I (Sm), and *Bgl*I (Bg). DNA fragments were separated in a 1% agarose gel with 0.5× TBE buffer (14 °C) at 6 V/cm, using a separation angle of 120°. Pulse time was ramped from 3 to 30 s for 24 h. Lanes: L, Lambda Ladder PFG Marker; M, MidRange I PFG Marker. Sizes (kb) of DNA fragments are indicated at left.

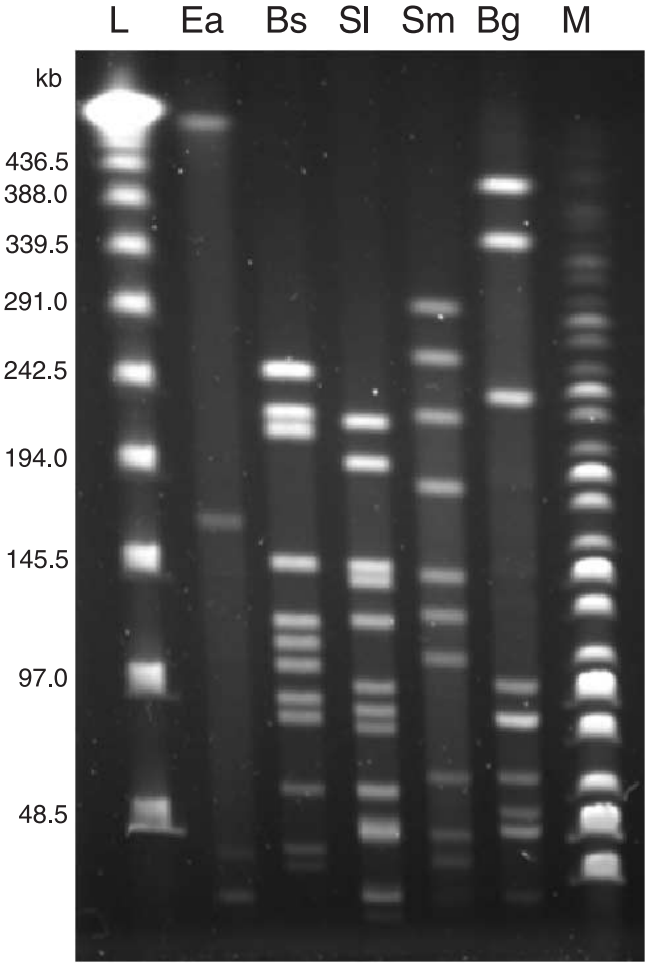

*Sma*I (CCCGGG), *Bss*HII (GCGCGC), *Bgl*I (GCCNNN NNGGC), and *Sal*I (GTCGAC). The number of DNA bands that could be detected on the PF gels after single digestions with these enzymes ranged from 3 to 15 (Fig. 1 and data not shown). Some bands represented multiple fragments, based on the intensity of their staining by ethidium bromide. For example, fragments E and F in the *Bgl*I digest formed a double band corresponding to co-migrating DNAs of about 85 kb (Fig. 1). In some cases, multiple fragments that formed a single band under one set of PF conditions could be separated by using different pulse and run times, making it possible to estimate the sizes of the fragments individually. In other cases, co-migrating fragments could not be resolved using one-dimensional PFGE. The sizes of fragments were averaged from the results of several PF gels run under different pulse and electrophoresis run times. Conventional agarose gel electrophoresis of total DNA extracted from *S. kunkelii* CR2-3x, and digested singly with *Bss*HII, *Sal*I, *Sma*I, or *Bgl*I, confirmed the sizes of bands <15 kb detected in PFGE and revealed the presence of three additional DNA bands less than 5 kb in the *Sal*I digest (data not shown). Fragments resulting from single digests of chromosomal DNA were designated by Apa, Eag, Bgl, Bss, Sal, or Sma and a letter, or a letter and number, to identify fragments resulting from digestions with the enzymes *Apa*I, *Eag*I, *Bgl*I, *Bss*HII, *Sal*I, or *Sma*I, respectively, (Table 2).

The size of the *S. kunkelii* CR2-3x chromosome was estimated by addition of the sizes of the restriction enzyme fragments (Table 2). DNA fragments determined, in a separate study using Southern hybridizations (data not shown), to represent plasmids were not included. The estimated size of the chromosome was 1550 kb, a result in close agreement with the size (1600 kb) estimated based on analyses of the undigested, linearized chromosome and the DNA digested with *Asc*I or I-*Ceu*I.

Analyses of double digestions and 2-D PF gels

To determine the chromosomal order of single enzyme restriction fragments, we used 2-D PFGE to separate DNA fragments obtained in sequential, reciprocal double enzyme digestions using *Apa*I, *Eag*I, *Bgl*I, *Bss*HII, *Sal*I, and *Sma*I in all possible pair combinations. An example of a typical gel is shown (Fig. 2). Linking fragments were identified by comparing identical DNA spots from the reciprocal digests on the 2-D gels and were assigned as overlapping on the chromosome map. Although it was not always possible to detect, in 2-D PF gels, small (<20 kb) DNA bands resulting from double enzyme digestions because of insufficient amounts of DNA, their presence could be deduced when the sum of sizes of the double digestion products was less than the size of the single fragment from which they were derived.

Construction of the physical map of the *S. kunkelii* CR2-3x chromosome

The physical map of the *S. kunkelii* CR2-3x chromosome (Fig. 3) was constructed after determining the linked, overlapping restriction fragments and the relative cleavage positions of the enzymes based on analyses of 2-D PF gels. Initially, the three Apa fragments were arbitrarily ordered and the three *Apa*I sites placed on the circular map. The fragments from the *Eag*I digests were then aligned with the Apa fragments. Two Eag fragments (A and C) were ordered with the three Apa fragments, and three *Eag*I sites were placed on the map, but the order of fragments Eag B and Eag D in the Apa A fragment could not be determined until additional analyses of 2-D PF gels with *Eag*I and *Bss*HII or *Sma*I. Using the data from 2-D PF gels and identification of linking fragments, the restriction fragments were aligned, and the cleavage sites from enzymes *Asc*I, I-*Ceu*I, *Sma*I, *Bss*HII, *Bgl*I, *Sal*I, and the fourth *Eag*I site were placed on the chromosome map.

Pairs of DNA fragments (Bgl E and Bgl F, Bgl I and Bgl J, and Sal I and Sal J) that had co-migrated in one-dimensional PFGE were resolved in 2-D PFGE and their positions mapped accurately on the chromosome.

Some of the smallest (<50 kb) DNA fragments resulting from *Sal*I digestion were difficult to position on the map.

Table 2. Size estimations of *Spiroplasma kunkelii* CR2-3x chromosomal DNA fragments generated by single digestion with selected

Restriction enzyme	Fragment designation and size (kb)										
*Asc*I or I-*Ceu*I	A										
	1600										
*Apa*I	A	B	C								
	1250	170	130								
*Eag*I	A	B	C	D							
	700	645	170	35							
*Bss*HII	A	B	C	D	E	F	G	H	I	J	K
	255	235	225	150	125	120	110	95	85	55	35
*Sma*I	A	B	C	D	E	F	G	H	I	J	K
	300	265	235	185	148	130	115	65	42	32	18
*Bgl*I	A	B	C	D	E	F	G	H	I	J	K
	425	365	240	100	85	85	65	50	45	45	28
*Sal*I	A	B	C	D	E	F	G	H	I	J	K
	230	200	150	145	127	100	90	80	55	55	48

*Fragments Sal S-1, Sal S-2, and Sal S-3 were detected and their sizes estimated by conventional agarose gel electrophoresis.

Fig. 2. One- and two-dimensional pulsed-field gel electrophoresis (PFGE) of *Spiroplasma kunkelii* CR2-3x genomic DNA digested with *Sma*I and (or) *Sal*I. (A) Two-dimensional PFGE of DNA digested with *Sma*I followed by *Sal*I; letters indicate individual *Sma*I fragments digested with *Sal*I. (B) One-dimensional PFGE of DNA digested with *Sal*I (Sl), *Sal*I and *Sma*I (D), or *Sma*I (Sm). (C) Two-dimensional PFGE of DNA digested with *Sal*I followed by *Sma*I; letters indicate individual *Sal*I fragments digested with *Sma*I. DNA fragments were separated in the first dimension as described for Fig. 1; for the second dimension, the pulse time was ramped from 1 to 25 s for 20 h.

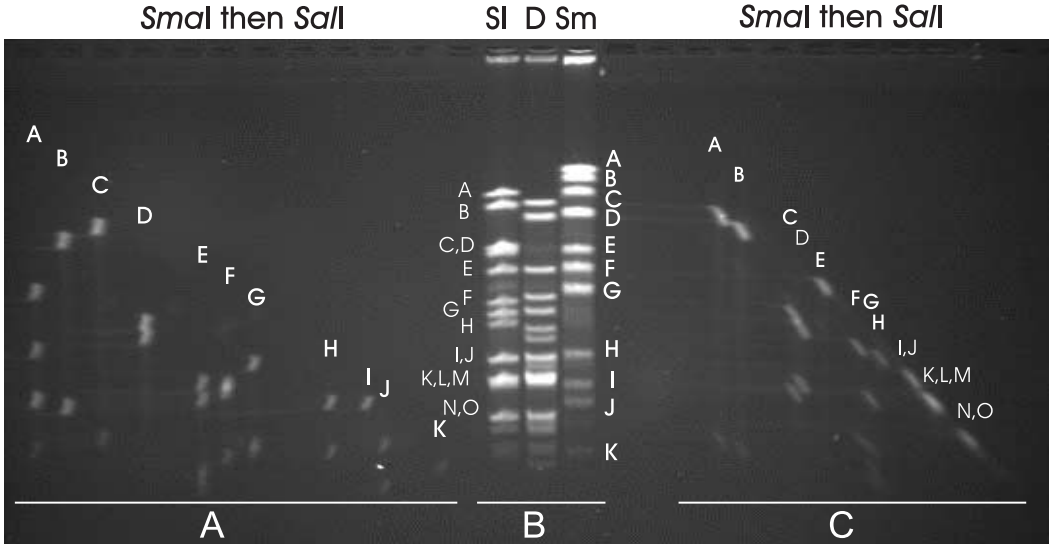

While the locations of fragments Sal K, Sal L, and Sal M-1 were later confirmed by hybridization experiments, as noted below, mapped positions of other Sal fragments (Sal M-2, Sal N, Sal O, Sal P, Sal Q, and Sal R) are tentative, since they could not be well-separated in 2-D gels; three fragments (<5 kb in size) were undetectable in 2-D PF gels and were omitted from the map.

The single *Asc*I site was arbitrarily chosen as the zero position of the map (Fig. 3). Although data from the PF gel analyses did not permit unambiguous location of the restriction sites for *Apa*I, *Bgl*I, *Sma*I, *Bss*HII, and *Sal*I that clustered near the *Asc*I site, examination of the *S. kunkelii* CR2-3x genome sequence data indicated that these sites were placed accurately on the map (Fig. 3).

Localization of genetic markers on the *S. kunkelii* chromosome

A partial genetic map of the *S. kunkelii* CR2-3x chromosome was constructed by determining the positions of 27 *S. kunkelii* chromosomal genes on the physical map. The genes, generally single copy in bacterial chromosomes, were identified in data from the *Spiroplasma kunkelii* Strain CR2-3x Genome Sequencing Project, and oligonucleotide pairs were designed to prime amplification of partial gene sequences

restriction endonucleases and detected by pulsed-field gel electrophoresis.

											Total size chromosome (kb)
											1600
											1550
											1550
L	M	N	O								
26	11	10	9								1546
											1535
L											
17											1550
L	M-1	M-2	N	O	P	Q	R	S-1*	S-2*	S-3*	
45	42	42	24	20	20	16	14	3.8	2	1.6	1511

from *S. kunkelii* DNA in PCR (Table 1). Of the 27 genes, 23 are involved in diverse cellular processes, including DNA replication and chromosome partitioning (*dnaA*, *gyrA*, *parC*, and *smc*); RNA transcription and protein translation (*rpoB*, *argS*, *leuS*, *thrS*, and *rrn*); carbohydrate, nucleotide, and co-enzyme metabolism (*amyA*, *gapN*, *gpm*, *eno*, *fruK*, *thyA*, *pnp*, *folD,* and *fhs*); membrane structure (*lemA* and spiralin gene); and protein secretion (*secY*, *secA*, and *ffh*). The remaining four genes encode proteins of unknown functions. Every PCR yielded a single DNA product, which was labeled for use as a hybridization probe.

The 27 gene probes were used in Southern hybridization analyses of chromosomal DNA digested singly with *Apa*I, *Eag*I, *Bgl*I, *Bss*HII, *Sal*I, and *Sma*I and separated by PFGE. The results of a typical PF gel and corresponding hybridization experiment are shown in Fig. 4. Results from the DNA hybridizations indicated that the probes were derived from single copy genes in the *S. kunkelii* CR2-3x chromosome.

Overlapping restriction fragments were identified and the genetic markers were located on the restriction map (Fig. 3). Each probe hybridized to a set of specific restriction fragments, and the approximate position of each gene was located on the chromosome within the boundaries of restriction sites that defined overlapping fragments; the 27 gene loci were widely distributed on the chromosome. In some cases, several genes mapped to an identical set of restriction fragments, but the gene order could not be precisely ascertained. For example, *ffh*, *amyA*, and *argS* each hybridized to fragments Eag A, Apa A, Bgl C, Sma A, Bss C, and Sal E, placing them within the area limited by the restriction site separating fragments Sal K and Sal E and the restriction site separating fragments Bss C and Bss J, but their precise order on the chromosome remains undetermined.

Spiroplasma kunkelii has a single ribosomal RNA (*rrn*) operon

The restriction fragment length polymorphism analysis showed that the chromosome of *S. kunkelii* CR2-3x contained a single restriction site for I-*Ceu*I (Fig. 3). This result was consistent with the presence of a single *rrn* operon in the *S. kunkelii* genome, since I-*Ceu*I is an endonuclease that recognizes a single, highly conserved 26 kb sequence found in the 23S rRNA genes of many bacteria (Liu et al. 1993). In addition, hybridizations with the *S. kunkelii* 16S-23S rDNA probe localized the operon to a single location on the chromosome spanning a recognition site for *Sal*I (Fig. 3). The probe derived from *S. kunkelii* 16S–23S rDNA hybridized with fragments Eag D, Apa A, Bgl K, Sma B, and Bss C and with two *Sal*I fragments, Sal K and Sal M-1. While the DNA sequence of the probe contained a single *Sal*I site but no sites for any other enzymes used in the mapping or the hybridization analyses, results of a query of the *S. kunkelii* Genome Sequencing Project database indicated that the complete *rrn* operon sequence also contained one site each for *Eag*I, I-*Ceu*I, and *Sma*I. These results permitted accurate placement of the single *rrn* on the chromosomal map at the junction of two *Sal*I fragments (Sal K and Sal M-1) (Fig. 3). The complete sequence of the *S. kunkelii* CR2-3x *rrn* operon was deposited in GenBank (accession No. DQ319068); gene order in the operon was 16S 23S 5S rRNA, an arrangement typical of bacterial *rrn* operons.

Discussion

In this study, the positions of 27 single copy genes were located on a detailed physical map of the *S. kunkelii* CR2-3x chromosome that was constructed by use of a combination of restriction enzyme analyses involving one- and two-dimensional PFGE and gene probe hybridizations of overlapping fragments to confirm the order of restriction fragments on the map. The estimated size of the strain CR2-3x chromosome (1550 kb) is in good agreement with chromosome sizes reported for other corn stunt spiroplasma strains, including strains E275 (1580–1610 kb) (Carle et al. 1995), I747 (1620 kb), and FL80 (1650 kb) (Barros 2002), and is within the size range (940–2220 kb) estimated for chromosomes of other spiroplasma species (Carle et al. 1995).

Of the eight restriction enzymes, having a total of 66 restriction sites detected on the CR2-3x chromosome map, *Apa*I and *Eag*I had fewer sites and *Bss*HII and *Sma*I had more sites than predicted based on base composition and chromosome size. Twenty-two recognition sites for *Sal*I were

Fig. 3. Physical and genetic map of the *Spiroplasma kunkelii* CR2-3x chromosome. Restriction enzymes *Apa*I, *Asc*I, *Eag*I, I-*Ceu*I, *Bss*HII, *Bgl*I, *Sal*I, and *Sma*I were used to construct the map. Radial lines indicate recognition sites for the enzymes. Letters designate individual fragments from enzyme digestion; fragment sizes are listed in Table 2. Tangential straight line segments indicate regions of the chromosome to which the single-copy genes were mapped. Gene designations are listed in Table 1. *oriC*, putative chromosomal origin of replication.

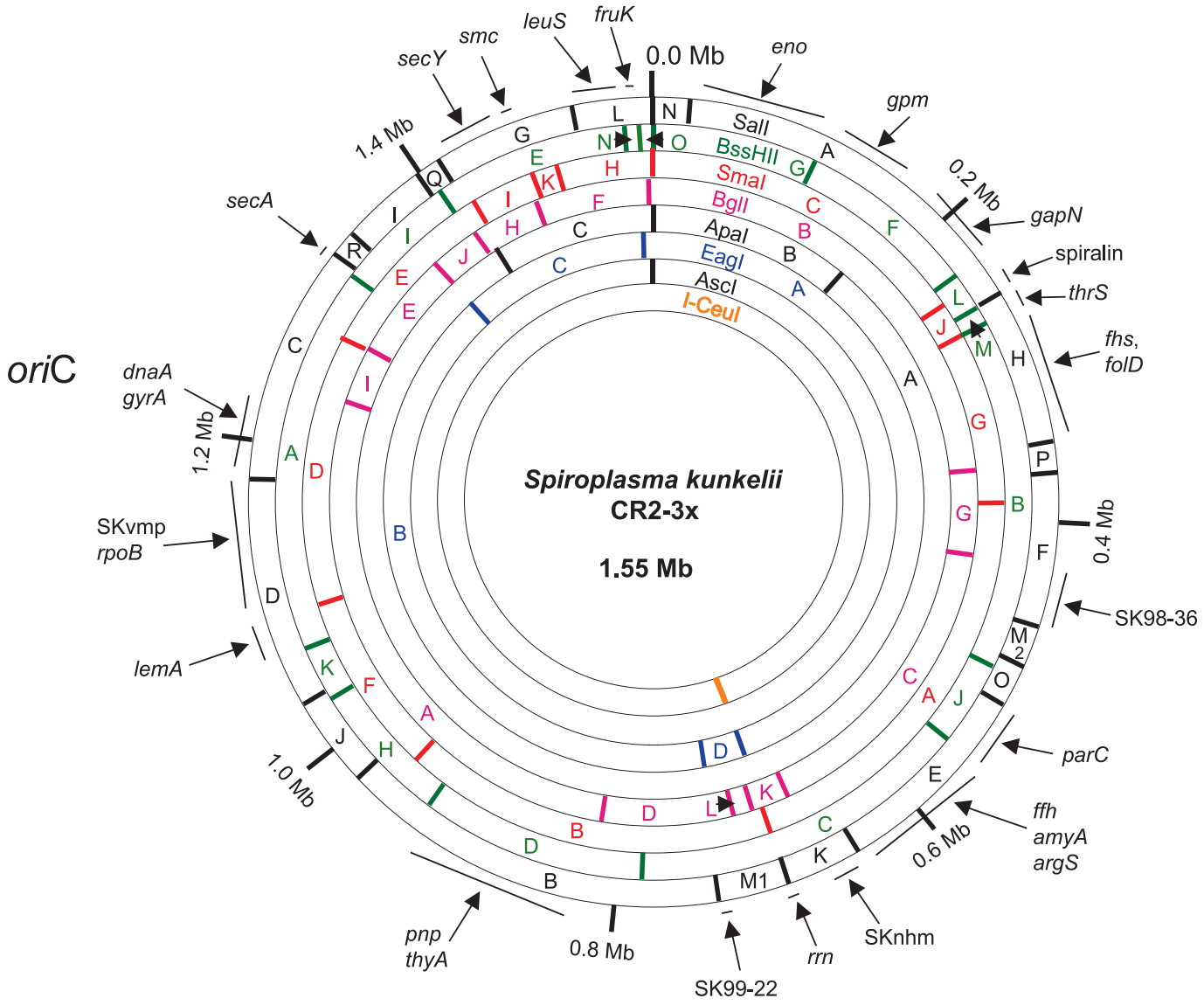

detected in the chromosome, representing only 37% of the predicted 62 cleavage sites, suggesting that some *Sal*I recognition sequences were not detected. One possibility is that DNA methylation may account for the relatively low number of *Sal*I sites detected in the *S. kunkelii* chromosome, as was suggested for *Spiroplasma melliferum* and *Spiroplasma citri* (Ye et al. 1992, 1994*a*, 1995). Ye et al. (1992) suggested that the majority of *Sal*I sites in the *S. citri* chromosome were part of a sequence that is methylated, blocking cleavage by this enzyme, and that *S. citri* strains may differ in the efficiency of their methylation systems (Ye et al. 1995). Interestingly, a search of the *Spiroplasma kunkelii* Strain CR2-3x Genome Sequencing Project database identified sequences that potentially encoded the three components of a type I restriction modification system, including genes for the restriction (*hsdR*), methylase (*hsdM*), and site-specificity (*hsdS*) components (this paper).

Sites for restriction enzymes having high G+C recognition sequences were unevenly distributed in the *S. kunkelii* CR2-3x chromosome. For example, 42% of all such sites were located in just 20% of the genome, from base positions 1250 to 25 kb on the chromosome map (Fig. 3). Other regions with clustered restriction sites included the areas from 215 to 280 kb and from 640 to 735 kb. The clustering of restriction sites may indicate that the G+C content is variable along the chromosome and that several regions have a higher G+C content than others. Clustering of high G+C restriction sites has been observed on the chromosome maps of other members of class *Mollicutes*, including mycoplasmas (Ladefoged and Christiansen 1992; Muto 1987; Pyle and

Fig. 4. Southern blot analysis of (A) *Spiroplasma kunkelii* CR2-3x genomic DNA digested with *Bss*HII (Bs), *Sma*I (Sm), and *Sal*I (Sl), and (B) hybridized with a spiralin gene probe. Electrophoresis was carried out as described in Fig. 1, except that the pulse time was ramped from 1 to 25 s for 20 h, followed by a ramped pulse time from 1 to 12 s for 12 h. DNA fragments (Sal A, Sma J, and Bss L) hybridizing with the probe were 230, 32, and 26 kb, respectively.

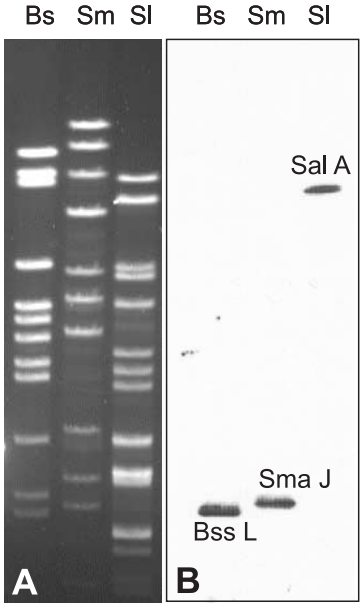

Finch 1988; Tola et al. 2001), phytoplasmas (Lauer and Seemüller 2000; Marcone and Seemüller 2001), and *S. citri* (Ye et al. 1992). Thus, interspersal of high G+C nucleotide sequence stretches among A+T-rich regions may be a common phenomenon in class *Mollicutes*.

Muto (1987) suggested that because of a biased mutational pressure to replace GC pairs with AT pairs, functionally less-important regions of a mycoplasma genome evolve faster and have a lower G+C content than functionally more-important regions. Thus, essential genes would have a higher G+C mol% content than other genes and a higher G+C mol% content than the genome overall. Therefore, regions where G+C-rich restriction sites are clustered may denote functional importance of the DNA in those regions (Muto 1987). Consistent with this hypothesis, 16S rRNA genes of some mollicutes have been reported in chromosomal regions that are high in G+C-rich restriction sites (Ladefoged and Christiansen 1992; Pyle and Finch 1988; Tola et al. 2001; Ye et al. 1992). The 16S rRNA gene of *S. kunkelii* is also located in a region high in G+C-rich restriction sites (this paper). In the present study, mapping the positions of *smc* and *secY* accurately located a previously studied 85 kb DNA fragment (Zhao et al. 2003) in a region of clustered G+C-rich restriction enzyme recognition sites in the *S. kunkelii* chromosome. This fragment has an overall base composition of 27.8 mol% G+C and potentially encodes genes that are functionally important for essential cell structures and processes, including translation and ribosome structure, DNA replication and chromosome segregation, regulation of transcription, and RNA processing. These findings and the location of the *S. kunkelii* 16S rRNA gene tend to support the hypothesis of Muto (1987).

Spiroplasma kunkelii is a member of spiroplasma group I (Davis and Lee 1982; Williamson et al. 1998). Previous studies have indicated that *Spiroplasma* spp. belonging to group I may possess one or two *rrn* operons (Amikam et al. 1984; Bové et al. 1989; Grau et al. 1990) and that some species in other groups may possess two copies of the *rrn* operon (Amikam et al. 1984; Bové et al. 1989). The present study indicates clearly that *S. kunkelii* CR2-3x possesses a single *rrn* operon and provides the first complete nucleotide sequence of the *S. kunkelii rrn* operon.

Identifying the positions of *dnaA* and *gyrA* on the *S. kunkelii* chromosome map indicated the location of the putative chromosomal origin of replication (*oriC*). The *oriC* region of bacterial chromosomes, and the organization of genes surrounding it, is highly conserved (Ogasawara and Yoshikawa 1992). In most Gram-negative bacteria, the gene order at the *oriC* is *dnaA dnaN recF gyrB*, and in Gram-positive bacteria, *gyrA* is linked to this region: *dnaA dnaN recF gyrB gyrA*. The organization of genes at the *oriC* region of mycoplasmas is generally similar to Gram-positive bacteria, but no *recF* has been found associated with this region (Razin et al. 1998; Zou and Dybvig 2002). A query of the *Spiroplasma kunkelii* CR2-3x Genome Sequencing Project database indicated that the gene order was *dnaA dnaN gyrB gyrA* (this paper), the same as reported by Ye et al. (1994*b*) for the *S. citri* chromosome.

In this communication, we present 26 new oligonucleotide pairs, designed on the basis of sequenced *S. kunkelii* genes, that were useful for amplification of gene sequences in the PCR. In addition to potential applications of the primers and amplified gene sequences as markers in future genetic mapping of other spiroplasma chromosomes, the primers significantly expand the potential for the use of multi-locus analyses in spiroplasma detection, identification, and phylogeny. To date, chromosomal physical and genetic maps have been published for only three *Spiroplasma* spp.: *S. citri* (Ye et al. 1992), *S. melliferum* (Ye et al. 1994*a*), and *S. kunkelii* (this paper). Direct comparisons of maps from different species may be premature, since considerable genome rearrangements have been reported even among diverse strains of *S. kunkelii* (Barros 2002) and *S. citri* (Ye et al. 1995). On the other hand, construction of the physical and genetic map of *S. kunkelii* CR2-3x is assisting on-going efforts to sequence the complete *S. kunkelii* genome by facilitating gap closure through ordering contigs on the chromosome and identifying sequences for design of primers used in PCR amplification of gap-spanning sequences. The completed *S. kunkelii* CR2-3x genome will lead to a better understanding of spiroplasma phylogeny and evolution within and across species.

Acknowledgements

We gratefully acknowledge Jonathan Shao for excellent technical assistance and Rasa Jomantiene for helpful discussions. *Spiroplasma kunkelii* genome sequence data were made available by Bruce Roe, ShaoPing Lin, HongGui Jia, HongMin Wu, and Doris Kupfer (University of Oklahoma, Department of Chemistry and Biochemistry, Norman, OK 73019, USA) and Robert E. Davis (US Department of Agriculture,

Agricultural Research Service, Molecular Plant Pathology Laboratory, Beltsville, MD 20705, USA).

References

Amikam, D., Glaser, G., and Razin, S. 1984. Mycoplasmas (*Mollicutes*) have a low number of rRNA genes. J. Bacteriol. **158**: 376–378.

Bai, X., Fazzolari, T., and Hogenhout, S.A. 2004*a*. Identification and characterization of *traE* genes of *Spiroplasma kunkelii*. Gene, **336**: 81–91.

Bai, X., Zhang, J., Holford, I.R., and Hogenhout, S.A. 2004*b*. Comparative genomics identifies genes shared by distantly related insect-transmitted plant pathogenic mollicutes. FEMS Microbiol. Lett. **235**: 249–258.

Barros, T.S.L. 2002. Caracterização molecular de mollicutes fitopatogênicos no Brasil. Tese de Doutorado, Universidade de Brasília, Brasília, Brazil.

Barros, T.S.L., Davis, R.E., Resende, R.O., and Dally, E.L. 2001. Design of a polymerase chain reaction for specific detection of corn stunt spiroplasma. Plant Dis. **85**: 475–480.

Bautsch, W. 1988. Rapid physical mapping of the *Mycoplasma mobile* genome by two-dimensional field inversion gel electrophoresis techniques. Nucleic Acids Res. **16**: 11461–11467.

Birren, B., and Lai, E. 1993. Pulsed field gel electrophoresis. A practical guide. Academic Press, New York.

Bové, J.M., Carle, P., Garnier, M., Laigret, F., Renaudin, J., and Saillard, C. 1989. Molecular and cellular biology of spiroplasmas. *In* The mycoplasmas. Vol. 5. Spiroplasmas, acholeplasmas, and mycoplasmas of plants and arthropods. *Edited by* R.F. Whitcomb and J.G. Tully. Academic Press, New York. pp. 243–364.

Carle, P., Laigret, F., Tully, J.G., and Bové, J.M. 1995. Heterogeneity of genome sizes within the genus *Spiroplasma*. Int. J. Syst. Bacteriol. **45**: 178–181.

Davis, R.E., and Lee, I.-M. 1982. Comparative properties of spiroplasmas and emerging taxonomic concepts: a proposal. Rev. Infect. Dis. **4**(Suppl.): S122–S128.

Davis, R.E., and Worley, J.F. 1973. Spiroplasma: motile, helical microorganism associated with corn stunt disease. Phytopathology, **63**: 403–408.

Davis, R.E., Worley, J.F., Whitcomb, R.F., Ishijima, T., and Steere, R.L. 1972. Helical filaments produced by a mycoplasma-like organism associated with corn stunt disease. Science (Washington, D.C.), **176**: 521–523.

Davis, R.E., Chen, T.-A., and Worley, J.F. 1981. Corn stunt spiroplasma. *In* Virus and viruslike diseases of maize in the United States. Southern Cooperative Series Bulletin 247 for Southern Regional Research Project S-70. *Edited by* D.T. Gordon, J.K. Knoke, and G.E. Scott. Ohio Agricultural Research and Development Center, Wooster, Ohio. pp. 40–50.

Davis, R.E., Dally, E.L., Jomantiene, R., Zhao, Y., Roe, B., Lin, S., and Shao, J. 2005. Cryptic plasmid pSKU146 from the wall-less plant pathogen *Spiroplasma kunkelii* encodes an adhesin and components of a type IV translocation-related conjugation system. Plasmid, **53**: 179–190.

Giménez Pecci, M.P., Oliveira, E., Resende, R.O., Laguna, I.G., Conci, L.R., Avila, A., Herrera, P., Galdeano, E., Virla, E., and Nome, C.F. 2002. Ocorrência de doenças causadas por molicutes e por virus em milho nas Provincias de Tucumán e de Córdoba na Argentina. Fitopatol. Bras. **27**: 403–407.

Grau, O., Laigret, F., and Bové, J.M. 1990. Analysis of ribosomal RNA genes in two spiroplasmas, one acholeplasma and one unclassified mollicute. Zentbl. Bakteriol. **20**(Suppl) : 895–897.

Hackett, K.J., and Clark, T.B. 1989. Ecology of spiroplasmas. *In* The mycoplasmas. Vol. 5. Spiroplasmas, acholeplasmas, and mycoplasmas of plants and arthropods. *Edited by* R.F. Whitcomb and J.G. Tully. Academic Press, New York. pp. 113–200.

Hruska, A.J., and Gomez Peralta, M. 1997. Maize response to corn leafhopper (Homoptera: Cicadellidae) infestation and achaparramiento disease. J. Econ. Entomol. **90**: 604–610.

Krause, D.C., and Mawn, C.B. 1990. Physical analysis and mapping of the *Mycoplasma pneumoniae* chromosome. J. Bacteriol. **172**: 4790–4797.

Ladefoged, S.A., and Christiansen, G. 1992. Physical and genetic mapping of the genomes of five *Mycoplasma hominis* strains by pulsed-field gel electrophoresis. J. Bacteriol. **174**: 2199–2207.

Lauer, U., and Seemüller, E. 2000. Physical map of the chromosome of the apple proliferation phytoplasma. J. Bacteriol. **182**: 1415–1418.

Lee, I.-M., and Davis, R.E. 1980. DNA homology among diverse spiroplasma strains representing several serological groups. Can. J. Microbiol. **26**: 1356–1363.

Lee, I.-M., and Davis, R.E. 1989. Serum-free media for cultivation of spiroplasmas. Can. J. Microbiol. **35**: 1092–1099.

Liu, S.-L., Hessel, A., and Sanderson, K.E. 1993. Genomic mapping with I-*Ceu* I, an intron-encoded endonuclease specific for genes for ribosomal RNA, in *Salmonella* spp., *Escherichia coli*, and other bacteria. Proc. Natl. Acad. Sci. U.S.A. **90**: 6874–6878.

Maniatis, T., Fritsch, E.F., and Sambrook, J. 1982. Molecular cloning: a laboratory manual. Cold Spring Harbor Laboratory, Cold Spring Harbor, N.Y.

Marcone, C., and Seemüller, E. 2001. A chromosome map of the European stone fruit yellows phytoplasma. Microbiology (Reading, U.K.), **147**: 1213–1221.

Muto, A. 1987. The genome structure of *Mycoplasma capricolum*. Isr. J. Med. Sci. **23**: 334–341.

Nault, L.R. 1990. Evolution of an insect pest: maize and the corn leafhopper, a case study. Maydica, **35**: 165–175.

Neimark, H., and Kirkpatrick, B.C. 1993. Isolation and characterization of full-length chromosomes from non-culturable plant-pathogenic *Mycoplasma*-like organisms. Mol. Microbiol. **7**: 21–28.

Nunan, L.M., Lightner, D.V., Oduori, M.A., and Gasparich, G.E. 2005. *Spiroplasma panaei* sp. nov., associated with mortalities in *Penaeus vannamei*, Pacific white shrimp. Int. J. Syst. Evol. Microbiol. **55**: 2317–2322.

Ogasawara, N., and Yoshikawa, H. 1992. Genes and their organization in the replication origin region of the bacterial chromosome. Mol. Microbiol. **6**: 629–634.

Oliveira, E., Resende, R.O., Giménez Pecci, M.P., Laguna, I.G., Herrera, P., and Cruz, I. 2003. Incidência de viroses e enfezamentos e estimativa de perdas causadas por molicutes em milho no Paraná. Pesqui. Agropecu. Bras. **38**: 19–25.

Pyle, L.E., and Finch, L.R. 1988. A physical map of the genome of *Mycoplasma mycoides* subspecies *mycoides* Y with some functional loci. Nucleic Acids Res. **16**: 6027–6039.

Razin, S., Yogev, D., and Naot, Y. 1998. Molecular biology and pathogenicity of mycoplasmas. Microbiol. Mol. Biol. Rev. **62**: 1094–1156.

Summers, C.G., and Stapleton, J.J. 2002. Management of corn leafhopper (Homoptera: Cicadellidae) and corn stunt disease in sweet corn using reflective mulch. J. Econ. Entomol. **95**: 325–330.

Tola, S., Idini, G., Rocchigiani, A.M., Rocca, S., Manunta, D., and Leori, G. 2001. A physical map of the *Mycoplasma agalactiae* strain PG2 genome. Vet. Microbiol. **80**: 121–130.

Wang, W., Wen, B., Gasparich, G.E., Zhu, N., Rong, L., Chen, J., and Xu, Z. 2004. A spiroplasma associated with tremor disease in the Chinese mitten crab (*Eriocheir sinensis*). Microbiology (Reading, U.K.), **150**: 3035–3040.

Wang, W., Gu, W., Ding, Z., Ren, Y., Chen, J, and Hou, Y. 2005. A novel spiroplasma pathogen causing systemic infection in the crayfish *Procambarus clarkii* (Crustacea: Decapod), in China. FEMS Microbiol. Lett. **249**: 131–137.

Whitcomb, R.F., Chen, T.A., Williamson, D.L., Liao, C., Tully, J.G., Bové, J.M., Mouches, C., Rose, D.L., Coan, M.E., and Clark, T.B. 1986. *Spiroplasma kunkelii* sp. nov.: characterization of the etiological agent of corn stunt disease. Int. J. Syst. Bacteriol. **36**: 170–178.

Williamson, D.L., Whitcomb, R.F., Tully, J.G., Gasparich, G.E., Rose, D.L., Carle, P., Bové, J.M., Hackett, K.J., Adams, J.R., Henegar, R.B., Konai, M., Chastel, C., and French, F.E. 1998. Revised group classification of the genus *Spiroplasma*. Int. J. Bacteriol. **48**: 1–12.

Woese, C.R., Maniloff, J., and Zablen, L.B. 1980. Phylogenetic analysis of the mycoplasmas. Proc. Natl. Acad. Sci. U.S.A. **77**: 494–498.

Ye, F., Laigret, F., Whitley, J.C., Citti, C., Finch, L.R., Carle, P., Renaudin, J., and Bové, J.M. 1992. A physical and genetic map of the *Spiroplasma citri* genome. Nucleic Acids Res. **20**: 1559–1565.

Ye, F., Laigret, F., and Bové, J.M. 1994*a*. A physical and genomic map of the prokaryote *Spiroplasma melliferum* and its comparison with the *Spiroplasma citri* map. C.R. Acad. Sci. Paris, **317**: 392–398.

Ye, F., Renaudin, J., Bové, J.M., and Laigret, F. 1994*b*. Cloning and sequencing of the replication origin (*ori*C) of the *Spiroplasma citri* chromosome and construction of autonomously replicating artificial plasmids. Curr. Microbiol. **29**: 23–29.

Ye, F., Laigret, F., Carle, P., and Bové, J.M. 1995. Chromosomal heterogeneity among various strains of *Spiroplasma citri*. Int. J. Syst. Bacteriol. **45**: 729–734.

Zhao, Y., Hammond, R.W., Jomantiene, R., Dally, E.L., Lee, I.-M., Jia, H., Wu, H., Lin, S., Zhang, P., Kenton, S., Najar, F.Z., Hua, A., Roe, B.A., Fletcher, J., and Davis, R.E. 2003. Gene content and organization of an 85-kb DNA segment from the genome of the phytopathogenic mollicute *Spiroplasma kunkelii*. Mol. Genet. Genomics, **269**: 592–602.

Zhao, Y., Hammond, R.W., Lee, I.-M., Roe, B.A., Lin, S., and Davis, R.E. 2004*a*. Cell division gene cluster in *Spiroplasma kunkelii*: functional characterization of *ftsZ* and the first report of *ftsA* in mollicutes. DNA Cell Biol. **23**: 127–134.

Zhao, Y., Wang, H., Hammond, R.W., Jomantiene, R., Liu, Q., Lin, S., Roe, B.A., and Davis, R.E. 2004*b*. Predicted ATP-binding cassette systems in the phytopathogenic mollicute *Spiroplasma kunkelii*. Mol. Genet. Genomics, **271**: 325–338.

Zhao, Y., Davis, R.E., and Lee, I.-M. 2005. Phylogenetic positions of '*Candidatus* Phytoplasma asteris' and *Spiroplasma kunkelii* as inferred from multiple sets of concatenated core housekeeping proteins. Int. J. Syst. Evol. Microbiol. **55**: 2131–2141.

Zou, N., and Dybvig, K. 2002. DNA replication, repair and stress response. *In* Molecular biology and pathogenicity of mycoplasmas. *Edited by* S. Razin and R. Herrmann. Kluwer Academic/Plenum Publishers, New York. pp 303–321.